Temperature Distribution Effects During Polymerization of Methacrylate-Based Monoliths

Igor Mihelič,[1] Tine Koloini,[1] Aleš Podgornik[2]

[1]*Faculty of Chemistry and Chemical Technology, University of Ljubljana, Aškerčeva 5, SI-1000 Ljubljana, Slovenia*
[2]*BIA Separations d.o.o., Teslova 30, SI-1000 Ljubljana, Slovenia*

Received 1 April 2002; accepted 8 July 2002

ABSTRACT: Monolithic stationary phases are becoming increasingly important in the field of liquid chromatography. Methacrylate-based monoliths are produced via free-radical bulk polymerization. The preparation of large-volume monoliths is a major problem because the intensive heat released during polymerization causes distortion of the porous monolithic structure. This work presents experimental measurements of temperature distributions during polymerization in moulds of different sizes and at various experimental conditions. A mathematical model for the prediction of temporal and spatial temperature distribution during the polymerization of methacrylate-based monolithic columns is introduced. The polymerization is described by an unsteady-state heat conduction equation with the generation of heat related to the general kinetics of polymerization. Predictions from the mathematical model are in good agreement with the experimental measurements at different experimental conditions. A method for construction of large-volume monolithic columns is presented and an attempt is made to adopt the developed mathematical model in annular geometry. © 2003 Wiley Periodicals, Inc. J Appl Polym Sci 87: 2326–2334, 2003

Key words: polymerization; macroporous polymers; modeling

INTRODUCTION

Methacrylate-based monoliths are a novel GMA-EDMA (polyglycidyilmethacrylate-ethylendimethacrylate)-based material used as a stationary phase in liquid chromatography. In contrast to conventional packed beds, the main advantage of methacrylate-based monolithic columns is their porous structure. Pores in such monoliths are open on both sides and highly interconnected, forming a flow-through network. Consequently, the entire mobile phase is forced to flow through the monolith, which results in a fast convective mass transfer between the stationary and mobile phase.[1] This is not the case for conventional porous particles where the mobile phase inside the pores is stagnant. One of the key features of GMA-EDMA monoliths is bimodal pore size distribution that enables low back pressure at high throughput together with a large surface area needed for high binding capacity. Because of the above-mentioned advantages, methacrylate-based monolithic columns have been applied in various areas. Especially small analytical and semipreparative monolithic columns were found suitable for extremely fast separations of large molecules.[2–10] However, the construction of large-volume preparative monolithic columns still represents a big challenge. Very few attempts have been described so far,[11,12] and only recently has an approach demonstrating chromatographic characteristics of large monolithic columns been introduced.[13]

The preparation of large-volume homogeneous monolithic columns is a very complex process because exothermic polymerization causes pronounced temperature nonhomogeneity that significantly affects the structure.[12] Thermally initiated radical bulk polymerization of monomer and porogene mixture results in a two-phase system: in a white-colored continuous solid monolith and in inert liquid porogens inside the porous structure of the monolith. To obtain monoliths with a reproducible and uniform structure, besides the initial composition, the temperature during polymerization should also be carefully controlled, since it significantly affects the porous structure.[12] In order to control the temperature, polymerization is performed in a thermostated water bath. However, polymerization is highly exothermic and therefore the occurrence of substantial temperature gradients in large moulds is inevitable. This fact represents the main reason for nonhomogeneous structure of large monolithic columns.[12] The possibilities of controlling the temperature inside large moulds are very limited during polymerization and therefore the temperature increase is determined by experimental conditions. These condi-

Correspondence to: T. Koloini (tine.koloini@uni-lj.si).
Contract grant sponsor: the Ministry of Education, Science, and Sport of the Republic of Slovenia; contract grant number: L2-1522-0158-99, PS-103-510, and L2-3529-1655-01.

tions are the composition of the reactant mixture, the temperature of the water bath, the shape and the diameter of the mould, and heat transfer coefficients on both sides of the mould. For a successful production of large columns, experimental conditions have to be methodically selected. In order to accomplish this, detailed knowledge about the polymerization kinetics and the heat transfer mechanism is essential. A combination of this knowledge and an appropriate mathematical model should enable prediction of temperature profiles during polymerization. Such a mathematical model would enable better understanding of the complex behavior, which would be of great importance in the development of preparative-volume monolithic columns.

This work presents experimentally measured temperature profiles and an attempt to describe the polymerization process with a simplified mathematical model employing the already developed global kinetic rate equation.[14]

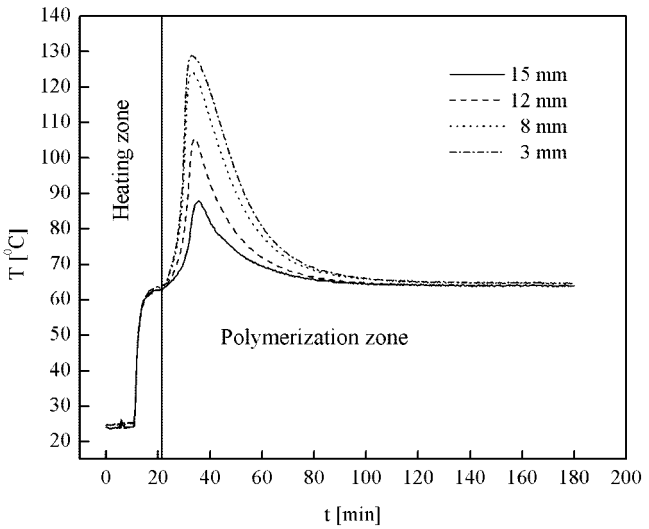

Figure 1 Temperature distributions at different radial positions during polymerization of methacrylate-based monolithic material in a 35 mm diameter cylindrical mould. Water bath temperature is 63°C. Radial positions of thermocouples are indicated.

EXPERIMENTAL

The reactant mixture consists of two monomers, 24% glycidyl-methacrylate and 16% ethylene-dimethacrylate, both from Aldrich (Steinheim, Germany); inert porogens, 12% dodecanol and 48% cyclohexanol; and an initiator, benzoyl peroxide-BPO, all from Fluka (Buchs, Switzerland).[12,15] This mixture forms a clear liquid that copolymerizes via a free-radical mechanism. The polymerization results in a two-phase system: a white-colored continuous solid monolith and an inert liquid porogens inside the porous structure of the monolith. The Trommsdorff effect is absent in this case, because the solution contains almost 60% inerts. Polymerizations were carried out in vertical stainless steel cylindrical moulds with diameters of 16, 35, 50, and 80 mm, respectively, and at water bath temperatures of 58, 63, 66, 68, and 70°C. All moulds had 1 mm thick walls and were 130 mm high. Sealed moulds were placed vertically in a thermostated water bath. The temperature inside the moulds was measured by standard Ni–CrNi thermocouples at different radial positions. The exact radial position of the thermocouples was measured with the precision of ±0.5 mm after the polymerization was completed. The acquisition of data from thermocouples was performed by a PC. The accuracy of the temperature measurements was experimentally estimated to ±1°C. Prior to the experiments, the reactant mixture was purged with a nitrogen for 15 min in order to strip out the dissolved oxygen that could influence the radical polymerization.

Specific heat capacity of the monolithic polymer was determined using differential scanning calorimetry (DSC) on the Mettler Toledo 821c differential scanning calorimeter. The experiments were conducted at atmospheric pressure in nitrogen atmosphere. Dynamic scans were taken at a heating rate of 10°C/min in the temperature range of 30–110°C. For the DSC sample preparation, approximately 10 mg of material was filled into an aluminum crucible of 40 μL with a perforated lid.

The mathematical model for the prediction of temporal and spatial temperature distributions during polymerization was written in Matlab (The Math Works Inc., Natick, MA). Numerical calculations and simulations were performed on a PC. Fitting of effective thermal diffusivity was performed by Mathematica (Wolfram Research Inc., Champaign, IL).

RESULTS AND DISCUSSION

Measurements of temperature distributions

A typical temperature distribution during polymerization inside the cylindrical mould of a 35 mm diameter at different radial positions is presented in Figure 1. The reactant mixture is prepared at room temperature and placed into a thermostated water bath at 63°C. Then the heating starts and the temperature of the reactant mixture gradually approaches the water bath temperature. This process is presented as the heating zone in Figure 1. At this point, the initiator becomes thermally unstable and starts to decompose to radicals that trigger radical polymerization. The highly exothermic polymerization causes rapid increase of temperature, which additionally accelerates the kinetics and consequently intensifies the heat release. This autoaccelerated process slows down when the kinetics becomes limited by the monomer concentration and

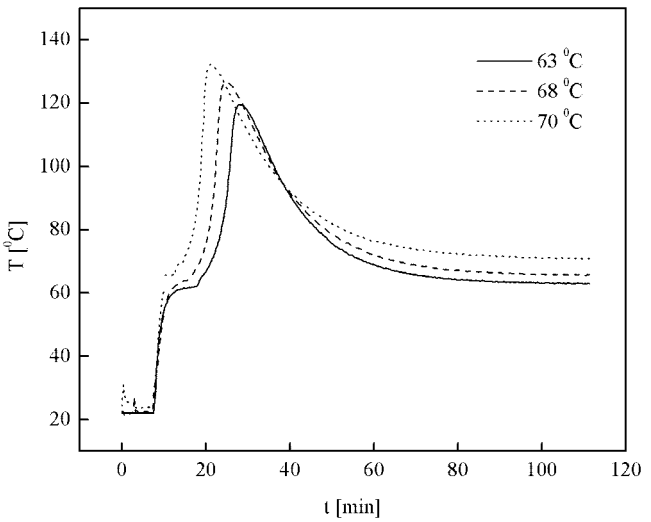

Figure 2 Comparison of experimentally measured temperature distributions at radial position of 9 mm during polymerization of methacrylate-based monolithic material in 35 mm diameter cylindrical moulds at different water bath temperatures.

eventually the polymerization ends. This process is presented as the polymerization zone in Figure 1. Here, in contrast to the heating zone, intensive temperature gradients in radial direction can be observed.

The polymerization can be carried out in moulds of different shapes and sizes and at different water bath temperatures. Figure 2 represents the comparison between temperature distributions at a fixed radial position for polymerization at different water bath temperatures. A pronounced influence of the water bath temperature on the polymerization kinetics and consequently on the maximal temperature is evident. Higher water bath temperature, according to the Arrhenius law, causes faster polymerization and a higher maximal temperature, altogether resulting in a less uniform porous structure of the monolithic column.[12] For this reason, a lower water bath temperature is preferred. However, the thermal stability of the initiator limits the use of low temperatures.

Mathematical model

The prediction of temporal and spatial temperature distributions during polymerization in closed moulds is a very difficult task. The main problem is the natural convective flow inside the mould caused by radial temperature gradients during polymerization. These convective flows enhance heat transfer that substantially influences the radial temperature distribution and the rate of polymerization. It is well known that these convective flows are very difficult to predict also in simple systems where the changes of physical and rheological properties are negligible.[16] Prediction of natural convection in complex systems, such as the polymerization presented, is at this moment still impossible to our knowledge but could be anticipated in the future with further development of computational fluid dynamics. However, convective contribution to heat transfer must therefore be simplified and included in the model. In this work, combined heat transfer is described as conduction only, where the effective conductivity incorporates the convective contribution through the relation[17]:

$$\lambda_{eff} = Nu_L \cdot \lambda \tag{1}$$

where Nu_L (conduction) = 1.

Since the Nu_L number is a function of the Rayleigh number and the aspect ratio (H/D), the effective conductivity is also a function of the aspect ratio. The lower the aspect ratio is, the higher the Nusselt number, which means that the convection intensity increases with diameter at the given mould height.

Considering the above-mentioned simplifications, the temperature distributions during polymerization in the mould can be mathematically described as unsteady-state heat conduction with generation of heat with the differential heat balance equation in cylindrical geometry:

$$\frac{\partial T}{\partial t} = \frac{\alpha_{eff}}{r}\frac{\partial}{\partial r}\left(r\frac{\partial T}{\partial r}\right) + \frac{\dot{S}}{\rho c_p} \tag{2}$$

For the solution of eq. (2), one initial and two boundary conditions are required. The initial condition is a uniform initial temperature distribution T_0. Justification of such initial condition has been experimentally confirmed and is presented in Figure 1, where the temperature at different radial positions, at the beginning of polymerization, is the same: $T = T_0$; $0 \le r \le R_0$; $t = 0$.

The first boundary condition assumes a symmetrical temperature profile around the center of the cylinder, while the second condition states that the temperature on the inner surface of the mould is equal to the temperature in the water bath:

$$\left.\frac{dT}{dr}\right|_{r=0} = 0 \quad r = 0 \quad t \ge 0$$

$$T = T_\infty \quad r = R_0 \quad t \ge 0$$

The second boundary condition has been experimentally verified by measuring the temperatures of the water bath and the temperatures on the outer and inner cylinder surface during the polymerization.

The term of heat flow in eq. (2) dictates the increase of the temperature during exothermal polymerization. The rate of heat generation depends on the kinetics and the heat of polymerization and can be written as

$$\dot{Q} = \frac{\dot{S}}{\rho} = \frac{dQ}{dt} \tag{3}$$

where the released heat Q is a linear function of the extent of reaction and equals the heat of polymerization at complete conversion:

$$Q = x(t, T)\Delta H_r \tag{4}$$

Since only thermal effects during the reaction are considered in the model, the global kinetic equation in terms of the extent of reaction and the value for the heat of polymerization are sufficient for the description of the process. Global kinetic parameters have been determined by DSC.[14] It has been shown that the global polymerization kinetics is of first order with $A = 1.681 \times 10^9\ s^{-1}$ and $E_{a,app} = 81.5$ kJ/mol, where the heat of polymerization is approximately 190 J/g. Therefore, the kinetic equation in terms of the extent of reaction can be written as

$$\frac{dx}{dt} = (1 - x)A \exp[-E_{a,app}/RT] \tag{5}$$

By integrating eq. (5), we obtain an expression for the calculation of the extent of reaction, which is a function of time and temperature:

$$x(t, T) = 1 - \exp\left[-A \int_0^t \exp[-E_{a,app}/RT]dt\right] \tag{6}$$

With a combination of eqs. (3), (4), and (6), and by inserting the solution for the heat flow into eq. (2), we obtain a mathematical expression describing the temperature profile during the polymerization in cylindrical geometry:

$$\frac{\partial T}{\partial t} = \frac{\alpha_{eff}(x)}{r} \frac{\partial}{\partial r}\left(r \frac{\partial T}{\partial r}\right) + \frac{1}{c_p(x)} \frac{\partial}{\partial t} \times \left(\Delta H_r\left(1 - \exp\left[-A \int_0^t \exp[-E_{a,app}/RT]dt\right]\right)\right) \tag{7}$$

In eq. (7), the specific heat capacity and the effective thermal diffusivity cannot be regarded as constants. The differences in physical properties of the liquid reagent mixture and the final two-phase product are very large. Therefore, the specific heat capacity in the mathematical model is considered as a linear function of the extent of reaction. The influence of specific heat capacity on the effective thermal diffusivity is much less pronounced than the influence of the effective conductivity, which depends on the radial temperature gradients. The exact correlation between the effective thermal diffusivity and the natural convective flows is not known, therefore an approximation has to be applied. A correlation between the effective thermal diffusivity and the extent of reaction is employed, because the radial temperature gradients are the largest in the first part of polymerization and the viscosity of the solution increases with the extent of reaction. For the sake of simplicity of the model, the effective thermal diffusivity is considered as a linear function of the extent of reaction:

$$\alpha_{eff}(x) = \alpha_0(1 - x) + x\alpha_f \tag{8}$$

$$c_p(x) = c_{p,0}(1 - x) + xc_{p,f} \tag{9}$$

where subscripts 0 and f denote initial and final values of thermal diffusivity and specific heat capacity. The specific heat capacity of porogens and of the reactant mixture was estimated to 2.1 J/gK, using literature data from SRC PhysProp Database (esc.syrres.com). The experimental estimation of specific heat capacity of the final two-phase system is rather difficult because of the pronounced endothermic effect caused by the evaporation of porogens at higher temperatures. Therefore, the specific heat capacity of monolithic material without vaporizable porogens inside the porous structure was measured using DSC analysis.[18] A sample of monolithic polymer was heated with a constant rate while heat flow (dH/dt) was recorded. Employing the experimental results in eq. (10), specific heat capacities at different temperatures were calculated:

$$c_p = -\frac{dH}{dt} \cdot \frac{1}{\eta} \cdot \frac{1}{m} \tag{10}$$

Figure 3 presents the results from DSC experiments for the determination of specific heat capacity of the monolithic polymer. The resulting specific heat capacity is slightly temperature-dependent, but for modeling purposes it can be regarded as a constant: $c_p = 1.2$ J/gK. Using the known mass proportions between monomers and porogens (40:60), the calculation of specific heat capacity of the two-phase system is straightforward and amounts to 1.74 J/gK.

The thermal diffusivity at the end of polymerization (α_f) was determined experimentally. Experiments were carried out by heating the cylindrical mould, containing the final two-phase mixture, in the thermostated water bath (Fig. 4). Temperatures at different radial positions were continuously recorded by the computer. Such experimental results can be mathematically described by eq. (1) without the heat flow term. The solution of such a simplified equation with a convection second boundary condition is analytical and is given as a Fourier series[17]:

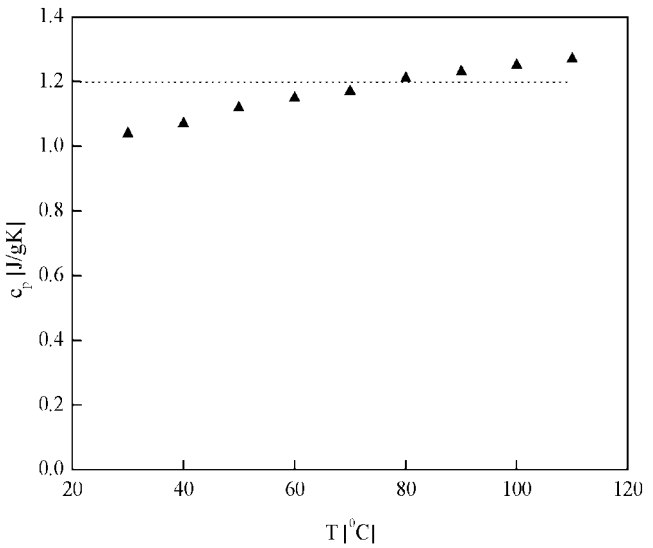

Figure 3 Dependence of the specific heat capacity of monolithic material on temperature. The dashed line presents the average value of the specific heat capacity used in the model.

$$\frac{T - T_\infty}{T_0 - T_\infty} = \sum_{i=1}^{\infty} C_i \exp[-\beta_i^2 \alpha t / R_0^2] J_0(\beta_i r / R_0) \quad (11)$$

where

$$C_i = \frac{2}{\beta_i} \frac{J_1(\beta_i)}{J_0^2(\beta_i) + J_1^2(\beta_i)} \quad (12)$$

and constants β_i are the roots of the algebraic equation

$$\frac{\beta_i J_1(\beta_i)}{J_0(\beta_i)} = Bi = \frac{h_\infty R_0}{\lambda} \quad (13)$$

The functions J_0 and J_1 are the Bessel functions of the first kind. In the present case, the solution is simplified because the value of the *Bi* number is large enough, so that the solution does not depend on the *Bi* number. Using measured temperature distributions at different radial positions in the cylindrical mould and fitting them with eq. (11), we obtain the values of thermal diffusivity for the two-phase system, which is $(0.7 \pm 0.2) \times 10^{-7}$ m^2/s. This value is a constant, regardless of experimental conditions and the mould aspect ratio, because the heat transfer mechanism in the two-phase system is mainly conduction. Here, the solid porous monolithic structure blocks the formation of noticeable convective flows that could substantially enhance the heat transfer. Figure 4 presents the comparison of the measured temperature profiles with numerical fits at several radial positions. Fitting was performed using the Levenberg–Marquardt method. A satisfactory convergence of the solution was achieved by applying the first eight terms of the Fourier series.

Determination of the initial thermal diffusivity is a much more difficult problem since the initial material in the mould is a liquid solution of monomers and porogens where the heat transfer is not only a conductive process, because it also includes free convection caused by spatial temperature gradients. Nevertheless, the empirical assessment of the value of initial thermal diffusivity is very difficult because it should incorporate the influence of the geometry of the mould. The only way to obtain this value for a given mould aspect ratio was to fit the experimental results of temperature distributions with eq. (7), where the only fitted parameter was α_0. The initial thermal diffusivity, once set for a given mould diameter, was then considered constant for that geometry. It has been determined that the value of initial thermal diffusivity increases with the mould diameter, which has been expected and is in accordance with literature data.[17]

The solution of the mathematical model was obtained using the finite difference method.[19] The convergence of the numerical solutions was tested. The increments Δt and Δr were adjusted according to the model stability and reasonable convergence demands considering the time needed for the computation. The numerical error of the computed results was estimated to be less then 1 K.

Figure 5 presents the comparison between experimentally measured temperature distributions and the mathematical model predictions for the polymerization in a 50 mm diameter cylindrical mould at water

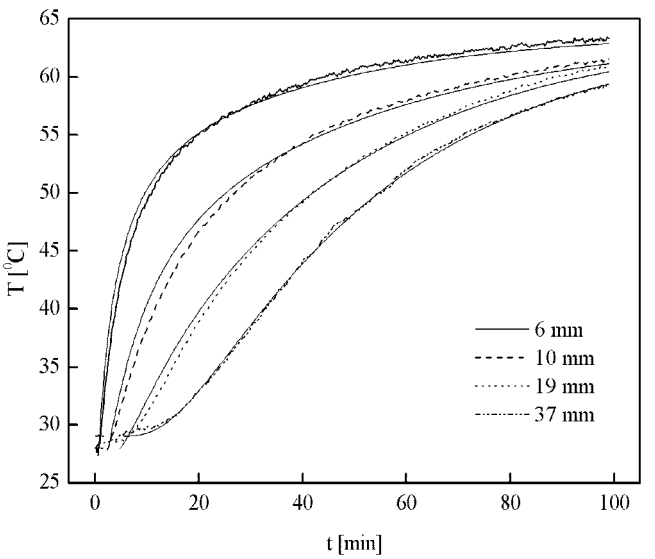

Figure 4 Comparison between measured temperature distributions and numerical fits at different radial positions. Experimental conditions: diameter of the mould, 80 mm; initial temperature, 28°C; temperature of the water bath, 64°C. Model parameters: R_0 = 40 mm; *Bi* = 100.

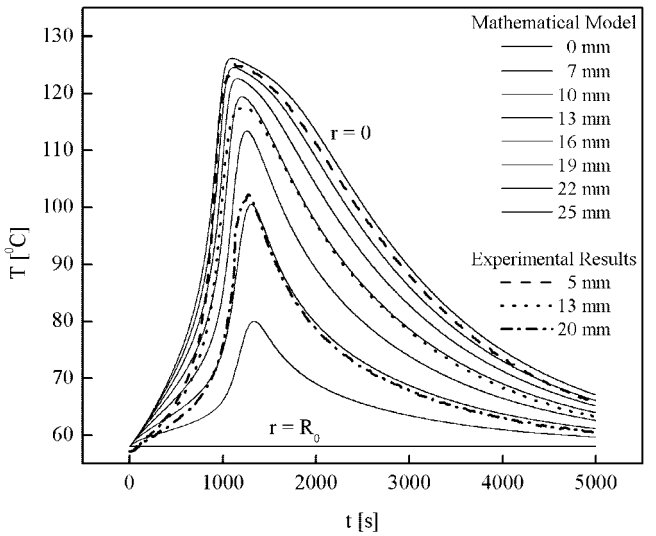

Figure 5 Comparison between experimentally measured temperature profiles and the mathematical model. Experimental conditions: cylindrical mould diameter, 50 mm; water bath temperature, 58°C. Model parameters: $c_{p,0} = 2.1$ J/gK; $c_{p,f} = 1.74$ J/gK; $\alpha_0 = 2.5 \times 10^{-7}$ m^2/s; $\alpha_f = 0.7 \times 10^{-7}$ m^2/s; $\Delta H_r = 190$ J/g; $T_0 = 58$°C; $T_\infty = 58$°C; $\Delta r = 0.5$ mm; $\Delta t = 0.5$ s. Radial positions of thermocouples are indicated.

bath temperature of 58°C. In Figure 6, a similar comparison for the polymerization in a 35 mm diameter cylindrical mould at the same water bath temperature of 58°C is presented. Both Figures 5 and 6 contain the calculated temperature profiles at different radial positions presented at regular intervals for better spatial

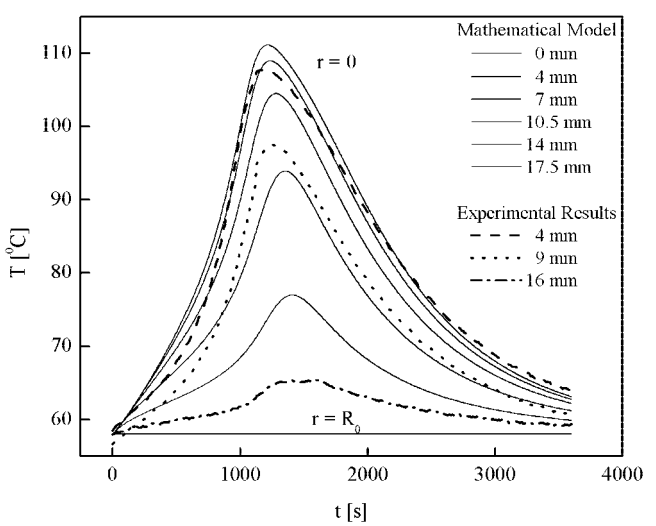

Figure 6 Comparison between experimentally measured temperature profiles and the predictions from the mathematical model. Experimental conditions: cylindrical mould diameter, 35 mm; water bath temperature, 58°C. Model parameters: $c_{p,0} = 2.1$ J/gK; $c_{p,f} = 1.74$ J/gK; $\alpha_0 = 1.3 \times 10^{-7}$ m^2/s; $\alpha_f = 0.7 \times 10^{-7}$ m^2/s; $\Delta H_r = 190$ J/g; $T_0 = 58$°C; $T_\infty = 58$°C; $\Delta r = 0.7$ mm; $\Delta t = 0.5$ s. Radial positions of thermocouples are indicated.

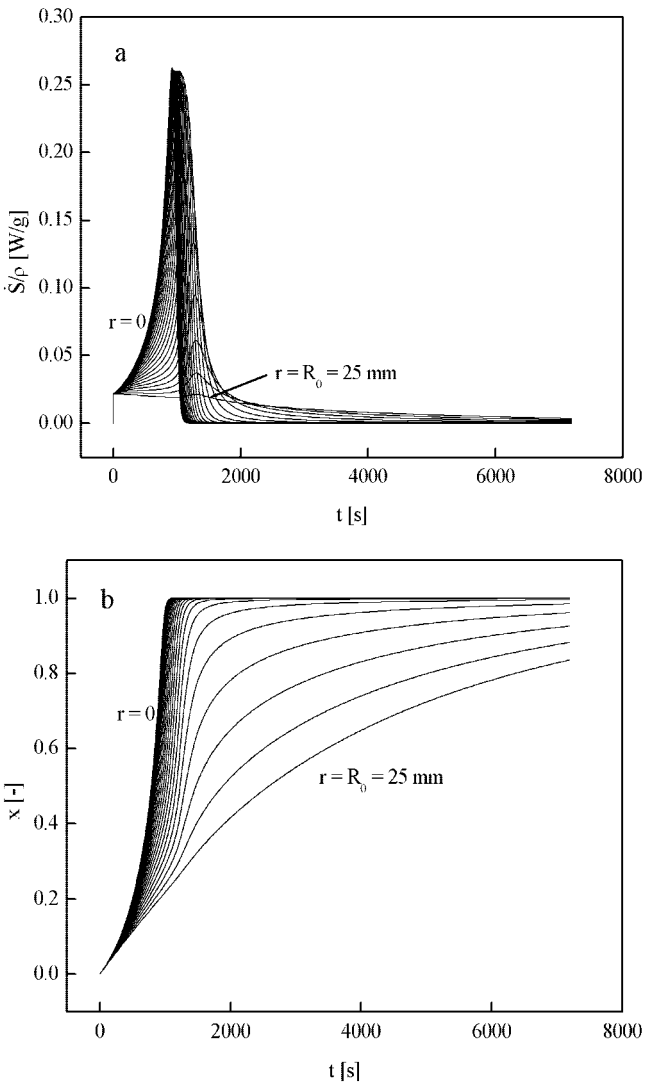

Figure 7 (a) Calculated rate of heat generation at different radial positions. The interval between the lines is equal to Δr, e.g., 0.5 mm. Model parameters are the same as in Figure 5.

representation. Good agreement of the mathematical model with the experimental data is evident from both these figures. The main difference between the two is in the maximal temperature achieved. In the case of the 50 mm diameter mould, the maximal temperature is 127°C, while in the case of the 35 mm diameter mould, it is only 111°C. This example clearly demonstrates the influence of the mould diameter on the maximal temperature during the polymerization.

The presented results show that the mathematical model for the prediction of temperature distributions during the polymerization of monolithic columns describes the process in a satisfactory manner. Therefore, it can be used for the prediction of the temperature and the conversion distributions for different experimental conditions and geometries of the moulds. In Figure 7, the calculated rates of generated heat and

TABLE I
Dependence of Effective Thermal Diffusivity on Cylindrical Mould Diameter

Mould Diameter (mm)	16	35	50	80
Effective thermal diffusivity $\times 10^7$ (m^2/s)	0.7	1.3	2.5	8

conversion profiles are presented. Since the presented profiles in Figure 7 were calculated using the same parameters as in Figure 5, the two figures can be compared.

It is evident from Figure 7 that very large differences in radial direction occur for the two profiles. By the time the polymerization in the center of the mould has been completed, the conversion near the wall reaches only 20%. This large radial dependence is reflected in the much longer time needed for the completion of polymerization than one would expect from the measured temperature profiles in Figure 5. Such observations show an evident advantage of the model.

With the presented mathematical model, it is also possible to predict the maximal temperature increase as a function of the mould diameter and water bath temperature. This information is very important for the production of homogeneous large-volume monolithic columns, where the maximal temperature increase is a critical parameter.[13] In order to predict the maximal temperature increase of an arbitrary mould diameter, the initial thermal diffusivity as a function of the mould diameter must be known. The dependence of the initial thermal diffusivity on the mould diameter was obtained by fitting the known values of the initial thermal diffusivity at experimental mould diameters (Table I) using a polynomial of the third order. The results presented in Figure 8 show the dependence of the theoretical maximal temperature increase at the center of the cylindrical mould on the diameter at different temperatures of the water bath. The dashed line indicates the maximal temperature increase at adiabatic conditions. This value was determined using the heat of reaction[14] ($\Delta Hr = 190$ J/g) and the average specific thermal coefficient ($c_p = 1.9$ J/gK) of the mixture throughout the polymerization. It should be noted that the results in Figure 8 represent a rough approximation of the real behavior.

Preparation of large-volume monolithic columns

A detailed analysis of polymerization kinetics and heat transfer during the polymerization showed an inevitable temperature increase, which can cause serious damage to the porous monolithic structure.[12] The scale-up is therefore limited by this factor, but there are several possibilities for the construction of large-volume monolithic columns. One method is further increasing of the diameter of short disk-shaped columns. Unfortunately, the mechanical instability and difficulties with uniform sample distribution over a large area limit the use of such units. Another possibility is the construction of long columns with small diameter. However, the very high pressure drop[20] becomes the main obstacle in a successful application of such units. An alternative approach that avoids these problems is a tube-shaped monolithic column.[13] Using this approach, the construction of an arbitrary-volume monolithic column is possible by inserting one tube of small thickness into another. However, joining of annuluses together represents another problem, and it is therefore essential to find the optimal annulus thickness. As a solution to this problem, the presented mathematical model has been adapted in order to describe the temperature distribution in an annular-shaped mould. This can be obtained by introducing new boundary conditions: $T = T_\infty$, $r = R_1$, $t \geq 0$; $T = T_\infty$, $r = R_2$, $t \geq 0$.

The solution of eq. (2) considering new boundary conditions presents the temperature distribution during the polymerization in an annular mould. The solution depends on annulus thickness and diameter and it approaches the solution for plate geometry for annuluses with large diameters where the curvature is small. Figure 9 presents the time sequence of one solution for an annular-shaped mould. It is evident here that the maximal temperature increase is not located in the center of the mould, as in the case of cylindrical moulds, but closer to the inner surface. Such behavior is expected and results from having different areas of the inner and outer surface available for heat transfer. Additionally, the sequences of conversion and generated heat flow profiles are presented in Figure 9.

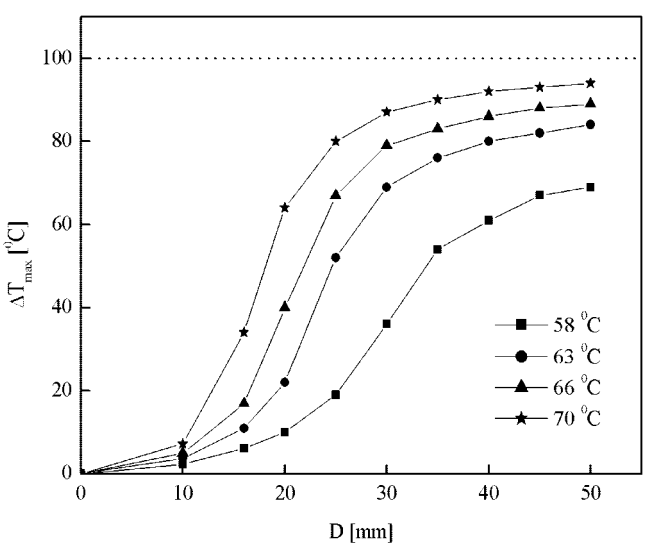

Figure 8 Dependence of the maximal temperature increase at the center of the cylindrical mould on cylinder diameter and on different water bath temperatures.

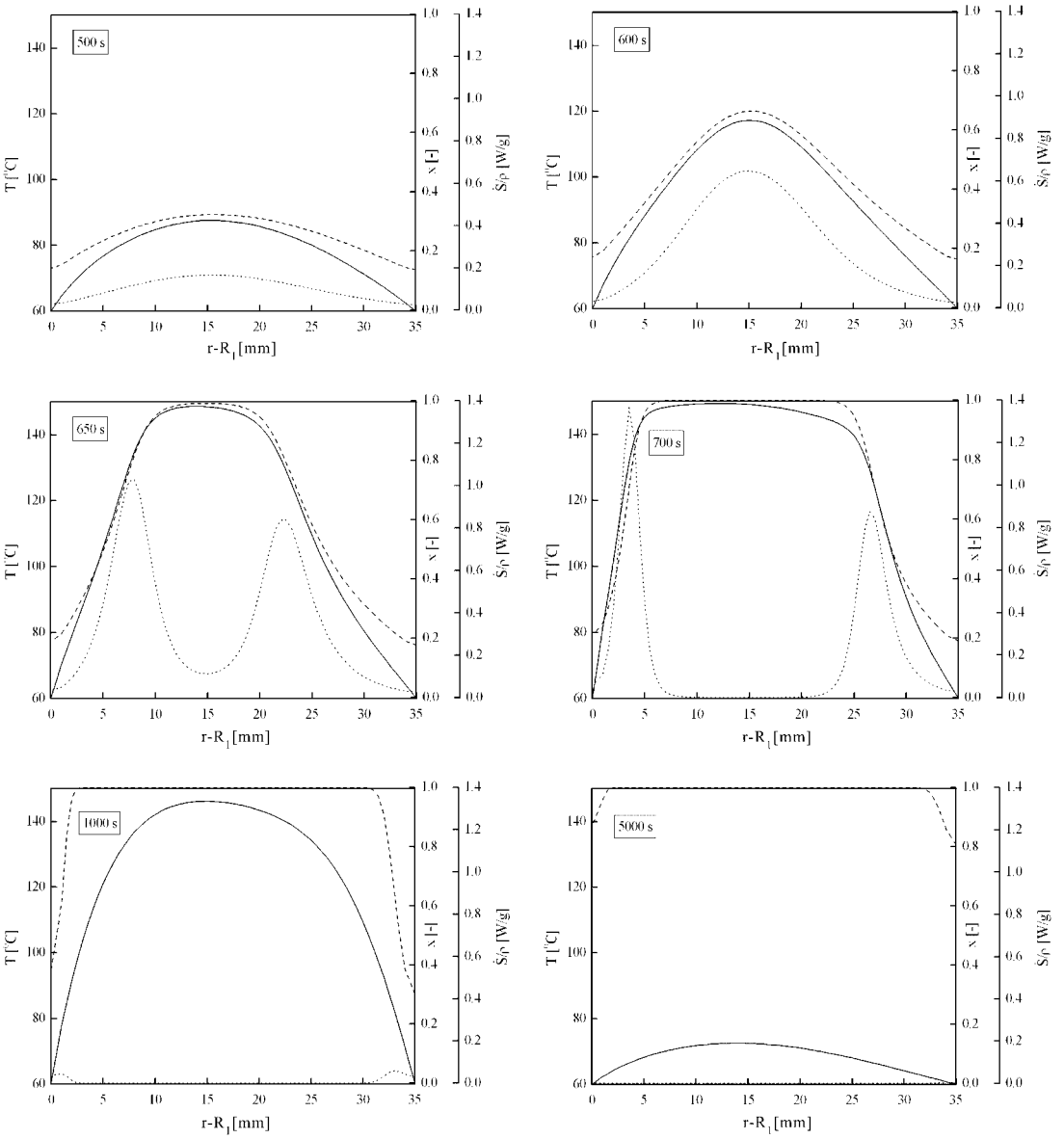

Figure 9 Time sequences of temperature, conversion, and generated heat flow distributions in an annular-shaped mould. Dimensions of the mould: $R_1 = 5$ mm; $R_2 = 40$ mm. Model parameters: $c_{p,0} = 2.1$ J/gK; $c_{p,f} = 1.74$ J/gK; $\alpha_0 = 2.5 \times 10^{-7}$ m^2/s; $\alpha_f = 0.7 \times 10^{-7}$ m^2/s; $\Delta H_r = 190$ J/g; $T_0 = 60$°C; $T_\infty = 60$°C; $\Delta r = 0.5$ mm; $\Delta t = 0.5$ s. Time scale is as shown. The solid line shows temperature distribution, the dashed line the conversion profile, and the dotted line the generated heat flow.

Although the results of the mathematical model for annular moulds are approximations, they provide important information about the process and could be useful in the development and preparation of homogeneous large-volume monolithic columns.

CONCLUSIONS

A mathematical model for the prediction of temperature distributions during the polymerization of methacrylate-based monolithic columns is presented. Using this model, good agreement with experimental results in cylindrical moulds has been achieved. Further development of large-volume monolithic columns focuses on the construction of monolithic units made of thin monolithic annuluses that can be joined together. This approach makes the construction of monolithic units of arbitrary volume theoretically possible. However, finding optimal conditions for polymerization in annular geometry is a complex problem, where the presented mathematical model, possibly with additional improvements, could be of great importance for further development of large-volume monolithic columns in the future.

NOMENCLATURE

A	preexponential factor (s^{-1})
Bi	Biot number (/)

C_i	constants in eq. (12)
c_p	specific heat capacity (J/gK)
D	inner cylinder diameter (m)
dH/dt	heat flow (W)
$E_{a,app}$	apparent activation energy (J/mol)
h_∞	external heat transfer coefficient (W/m^{2}K)
H	cylinder height (m)
ΔH_r	heat of reaction (J/g)
m	mass (g)
Nu_L	Nusselt number (/)
Q	released heat per unit mass (J/g)
$\dot{Q}$	released heat flow per unit mass (W/g)
r	cylindrical coordinate (m)
R_0	internal cylinder radius (m)
R_1	inner annulus radius (m)
R_2	outer annulus radius (m)
R	gas constant (J/molK)
$\dot{S}$	released heat flow per unit volume (W/cm^3)
T	temperature (°C)
T_0	initial temperature (°C)
T_∞	water bath temperature (°C)
t	time (s)
x	extent of reaction (/)
α_{eff}	effective thermal diffusivity (m^2/s)
β_i	constants in eq. (12)
λ_{eff}	effective thermal conductivity (W/mK)
λ	thermal conductivity (W/mK)
η	heating rate (°C/s)
ρ	density (g/cm^3)

References

1. Iberer, G.; Hahn, R.; Jungbauer, A. LC-GC 1999, 17, 998.
2. Josić, D.; Štrancar, A. Ind Eng Chem Res 1999, 38, 333.
3. Štrancar, A.; Koselj, P.; Schwinn, H.; Josić, D. Anal Chem 1996, 68, 3483.
4. Josić, D.; Schwinn, H.; Štrancar, A.; Podgornik, A.; Barut, M.; Lim, Y. P.; Vodopivec, M. J Chromatogr A 1998, 803, 61.
5. Giovannini, R.; Freitag, R.; Tennikova, T. B. Anal Chem 1998, 70, 3348.
6. Branović, K.; Buchacher, A.; Barut, M.; Štrancar, A.; Josić, D. J Chromatogr A 2000, 903, 21.
7. Podgornik, H.; Podgornik, A.; Perdih, A. Anal Biochem 1999, 272, 43.
8. Vodopivec, M.; Podgornik, A.; Berović, M.; Štrancar, A. J Chromatogr Sci 2000, 38, 489.
9. Podgornik, A.; Barut, M.; Jančar, J.; Štrancar, A.; Tennikova, T. B. Anal Chem 1999, 71, 2986.
10. Merhar, M.; Podgornik, A.; Barut, M.; Jakša, S.; Žigon, M.; Štrancar, A. J Liq Chromatogr 2001, 24, 2429.
11. Štrancar, A.; Barut, M.; Podgornik, A.; Koselj, P.; Schwinn, H.; Raspor, P.; Josić, D. J Chromatogr A 1997, 760, 117.
12. Peters, E. C.; Švec, F.; Fréchet, J. M. J. Chem Mater 1997, 9, 1898.
13. Podgornik, A.; Barut, M.; Štrancar, A.; Josić, D.; Koloini, T. Anal Chem 2000, 72, 5693.
14. Mihelič, I.; Krajnc, M.; Podgornik, A.; Koloini, T. Ind Eng Chem Res 2001, 40, 3495.
15. Švec, F.; Fréchet, J. M. J. Chem Mater 1995, 7, 707.
16. Stiles, P. J.; Fletcher, D. F. Phys Chem Chem Phys 2001, 3, 1617.
17. White, F. M. Heat Transfer; Addison-Wesley: London, 1984.
18. Turi, A. Thermal Characterization of Polymeric Materials; Academic Press: San Diego, 1997.
19. Riggs, J. B. An introduction to numerical methods for chemical engineers; Texas Tech University Press: Texas, 1988.
20. Švec, F.; Fréchet, J. M. J. J Chromatogr 1995, 702, 89.